OPTIMIZATION OF SPOILER THICKNESS FOR TOTAL BODY IRRADIATION (TBI) UTILIZING TOMOTHERAPY TECHNOLOGY

A Dissertation
Presented to
The Academic Faculty

by

Bashar Ziadat

In Partial Fulfillment
of the Requirements for the Degree
Master of science in Medical Physics in
GEORGIA INSTITUTE OF TECHNOLOGY/COLLEGE OF ENGINEERING

Georgia Institute of Technology
August 2024

OPTIMIZATION OF SPOILER THICKNESS FOR TOTAL BODY IRRADIATION (TBI) UTILIZING TOMOTHERAPY TECHNOLOGY

Approved by:

Dr. C-K Chris Wang, Advisor
School of [Mechanical Engineering]
Georgia Institute of Technology

Dr. Steven Biegalski
School of [Mechanical Engineering]
Georgia Institute of Technology

Dr. Farshad Mostafaei
Department of Radiation Oncology
Augusta University

Dr. chulhaeng Huh
Department of Radiation Oncology
Augusta University

Date Approved: May 09, 2024

ACKNOWLEDGEMENTS

I would like to especially thank my advisor Dr. Wang for his guidance and support, Dr. Biegalski for always answering my question whether they are academic or administrative, Dr. Huh, and Dr. Mostafaei for letting me use their equipment and their guidance and support.

TABLE OF CONTENTS

LIST OF TABLES

LIST OF FIGURES

SUMMARY

Delivering total body irradiation (TBI) with a Tomotherapy unit presents a unique challenge: minimizing lung dose while achieving a high skin dose. Acrylic spoilers offer a potential solution by slightly attenuating the incident photon beam, and therefore, reduce the lung dose. The spoilers can also increase the skin dose by producing electrons via Compton scattering interactions of the incident photon beams. This study aimed to identify the optimal spoiler thickness for clinical application for TBI with a Tomotherapy unit. The dosimetric effects of these spoilers were investigated computationally and experimentally.

The results of this study show that, among the various thicknesses (0.0, 0.635, 0.953, and 1.588 cm) of the spoiler), the thickest (i.e. 1.588 cm) spoiler yielded the lowest lung dose and the highest skin dose. This conclusion is further supported by the experimentally obtained dose data from the EBT3 films that were mounted on the ArcCHECK phantom and irradiated with the Tomotherapy machine. The ion chamber measurements within the ArcCHECK system demonstrated good agreement with the TPS calculations, exhibiting a maximum error of only 0.5% for lung dose. Furthermore, the dose data measured with the ion chamber also show that lowest lung dose was achieved with the thickest spoiler.

CHAPTER I. INTRODUCTION

1.1 Background on large-field radiotherapy

There has been a renewed interest in large-field radiotherapy (LFR) especially for malignant diseases in the last decade. LFR has been challenging for medical physicists and radiation therapists due to many constraints. Specifically, the topic of interest has been on the various methods for total-body irradiation (TBI) and half-body irradiation (HBI) to try to overcome the constraints that are associated with this kind of treatment. The use of large fields to treat patients would result in uncertainties in the absolute dosimetry and a big dose variation throughout the body due to different amount of attenuation of radiation in the different tissues in the body and the nature of the radiation dose profile where no flattening filter is used.

LFR has been clinically implemented in different ways where TBI and HBI would have different dose fractionations with different dose rates. These include high-dose-rate (HDR) TBI, low-dose-rate (LDR) TBI, half body irradiation (HBI), and total lymphoid irradiation (TLI). The HDR TBI has been used to suppress the immune system for patients to receive procedures such as the bone marrow transplant (BMT)[1, 2]. The LDR TBI has been used to reduce the lung complications in treating lymphocytic leukemia, lymphomas and neuroblastoma[2, 3, 4, 5]. The HBI has been used to treat Ewing's sarcoma[6] and the palliation of wildly metastasized diseases[7], and for ovarian ablation (OA) to stop or reduce the production of estrogen[8]. Lastly, TLI is used to irradiate the lymphatic system as a complimentary immunosuppressant for patients who face allograft rejection[9]. TLI can also

be used to treat a number of autoimmune diseases such as multiple sclerosis, aplastic anemia, rheumatoid arthritis, and systemic lupus erythematosus[9].

Acute side effects of TBI can significantly impact a patient's quality of life during treatment[4,5,7]. These include nausea, vomiting, diarrhea, mucositis (inflammation in the mouth and gastrointestinal tract)[2], and skin reactions. Additionally, TBI can increase the risk of secondary malignancies, organ dysfunction, and impaired fertility.

For these reasons, research has focused on refining TBI techniques and reducing treatment-related toxicities[4,5,7,8]. This has been achieved through advancements in treatment planning algorithms, improved radiation delivery technology, and enhanced supportive care strategies. These developments aim to improve the therapeutic ratio of TBI, maximizing the dose delivered to the tumor while minimizing the dose to healthy tissues.

1.2 Specifics on conventional TBI clinics

TBI clinics can be divided into two categories depending on the design and methods. The first category includes dedicated facilities that are specifically designed for LFR[2]. These facilities use one or more gamma-emitting radioactive sources of Co-60 and Cs-137 to create large radiation field for TBI. It was found that a minimum four sources are needed to achieve a uniform distribution of the dose for irradiating the whole body[1,2]. Figure 1 is a visual representation of a four-source irradiation method for TBI. The second category includes facilities originally built for linac-based conventional radiotherapy treatments but were modified to produce very large radiation fields to accommodate TBI. The modifications include gantries having extended rotation ranges, collimators capable of

shaping large fields, and couches that can accommodate patients in various positions for LFR[2]. Figure 2 shows a geometric configuration of a linac-based treatment for TBI.

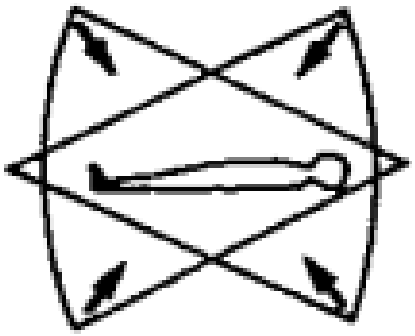

Figure 1. A visual representation of a four-source irradiation method, where two sources would be above the patient and two would be below the patient.[2]

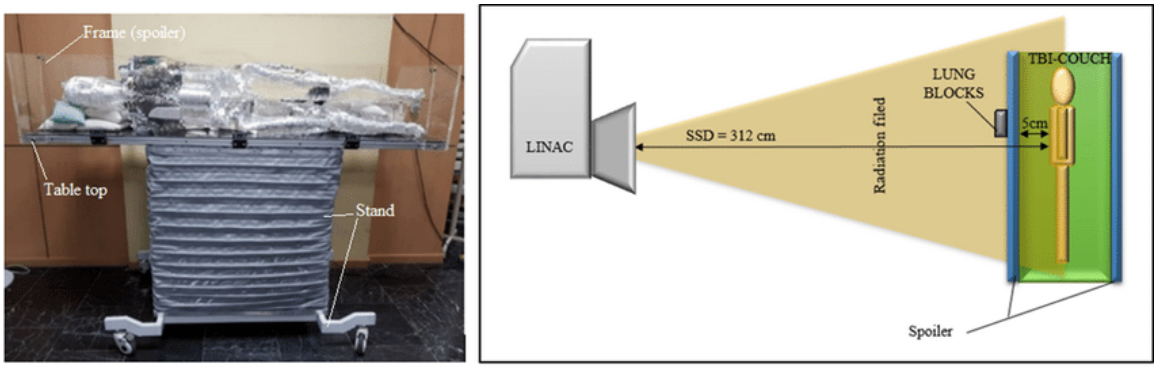

Figure 2. Total body irradiation (TBI) setup for Linac-based AP/PA geometry: (a) lateral view of the phantom on a specifically constructed TBI couch including tabletop, stands, and therapeutic frame, in the treatment room; (b) position of linear accelerator (LINAC), phantom, lung bocks, TBI couch, and radiation field.[7]

1.3 Advantages of using Tomotherapy machine for TBI

Lately, several clinics have started using Tomotherapy machine for TBI[8]. Figure 3 shows the Tomomachine and its components. While Tomomachine is a linac-based system, it offers several advantages over the conventional linac-based systems for TBI. The advantages include the ability to deliver a conformal and homogeneous dose distribution coupled with improvement in organ sparing, image-guided delivery, and potentially reduced treatment time.

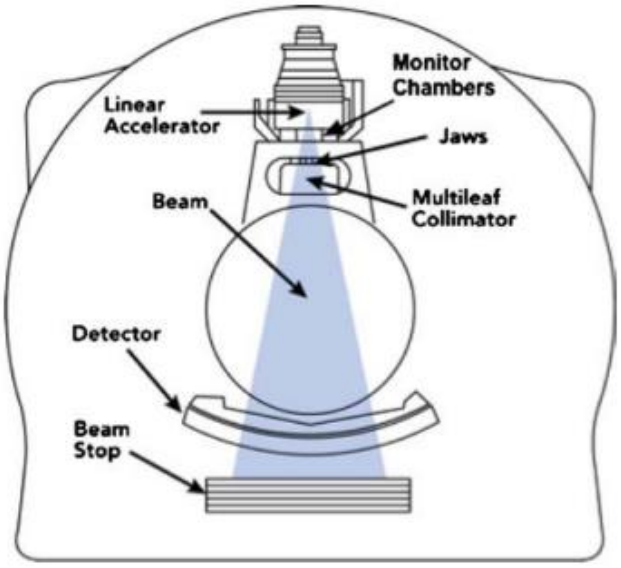

Figure 3. Tomomachine and its components

Combining a moving linear accelerator with a modulated fan beam allows for continuous treatment delivery throughout gantry rotation, enabling the Tomomachine to conform the beam to complex patient anatomy, particularly in areas like the head and neck or pelvis. This conformal dose delivery reduces unwanted dose variations (hotspots and

coldspots) commonly observed with conventional techniques, leading to a more homogeneous dose distribution across the target volume.

Furthermore, Tomotherapy's precise beam modulation capabilities allow for sculpting the dose around critical organs like the lungs[9], heart, and kidneys, which are particularly vulnerable to radiation damage during TBI. By minimizing dose exposure to these organs, Tomotherapy has the potential to reduce the risk of both acute and late toxicities associated with TBI, such as pneumonitis, pericarditis, and renal failure.

Additionally, Tomotherapy integrates cone-beam CT capabilities within the treatment workflow. This enables real-time patient positioning verification and potential tumor tracking during treatment delivery. This image-guided approach minimizes the impact of patient setup variations and potential organ motion, ensuring accurate delivery of the planned dose distribution to the target volume.

Finally, compared to conventional TBI techniques that require multiple static field deliveries, Tomotherapy offers the potential for shorter treatment times. This continuous delivery approach translates to decreased patient discomfort and potentially improved overall treatment experience.

1.4 Rationales and goals of this study

Regardless of the dose delivery methods used in a TBI treatment, the maximum dose along the beam path typically occurs at 1-2 cm depth in the patient. In fact, the skin dose is significantly lower than the dose deep inside the patient. While this skin-sparing effect is desirable for conventional radiotherapy, it is not desirable for TBI. To avoid skin sparing

for TBI, a common method is to place a spoiler in the beam path between the gamma or X-ray source and the patient[5,1]. The spoiler is usually a 1-2 cm thick plate made from a plastic material such as acrylic. The electrons produced via Compton scattering events occurring in the spoiler would increase the skin dose to the patient, and therefore increase the skin dose and avoid skin sparing. In other words, adding a spoiler helps increase the uniformity of the dose distribution in the patient and improves overall outcome of the TBI treatment. When using the LFT facilities for TBI, the spoiler is usually placed 20-30 cm away from the patient[1,2]. Because of the unique geometric configuration of the Tomomachine dose delivery system, the spoiler to be used with the Tomomachine for TBI must take the shape of a cylindrical ring.

This study aims to investigate how the spoiler's thickness impacts the dose uniformity and the dose to critical organs in a patient for clinical application for TBI with a Tomotherapy unit. The goal was to identify the optimal spoiler thickness by evaluating the dosimetric effects of the spoilers of various thicknesses both computationally and experimentally.

CHAPTER II. METHODOLOGY

The methodology of this study includes the use of several computational and experimental tools. The computational tools include the Monte Carlo radiation transport code, TOPAS[10,11,12], and the standardized digital phantoms representing a 15-year-old and a 35-year-old male. The digital phantoms were obtained from the National Institutes of Health (NIH)[13, 14] . The experimental tools include the ArcCHECK phantom/detector array[15, 16], the EBT 3 radiochromic film[17, 18], the film scanner[19], and a set of cylindrical ring spoilers (made from acrylic)[20] of various thicknesses. The experiment was conducted at the Tomotherapy unit of the Augusta University Radiation Oncology Department in Augusta, Georgia at the Georgia Radiation Therapy Center. The sections below first describe the details involved in computational evaluation of dose distributions in the various phantoms and then the details of experimental measurements.

2.1 Computational evaluation of dose distribution in phantoms

2.1.1 Computational tools

To evaluate the dose distribution within the patient for different spoiler thicknesses, Monte Carlo (MC) simulations were performed. Standardized digital phantoms representing a 15-year-old and a 35-year-old male were obtained from the National Institutes of Health (NIH) repository[13,14]. These phantoms provide realistic anatomical representations for simulating radiation transport within the human body.

The Monte Carlo radiation transport code, TOPAS[10,11], were used to model the entire Tomotherapy treatment geometry. TOPAS leverages the robust capabilities of the

GEANT4 toolkit[11, 12] to model complex geometries encountered in radiation therapy systems, including the linear accelerator (Linac), and multileaf collimator (MLC). The phantoms were meticulously positioned within the modeled geometry to mimic the patient setup during clinical treatment. TOPAS allows for accurate simulation of particle interactions (photons) with the various treatment components and the phantoms. This enables the calculation of absorbed dose within the phantoms, providing a comprehensive evaluation of dose distribution for different spoiler thicknesses.

2.1.2 TOPAS Simulation

To evaluate how spoiler thickness affects dose distribution in patients undergoing TBI, the TOPAS input data file included a detailed model replicating the actual Tomotherapy treatment geometry. This virtual environment allowed one to precisely define various components crucial for accurate dose calculations. The TOPAS input file also included defining the "source term", which was based on the X-ray beam characteristics of the Tomotherapy machine having the energy spectrum of a 6 MV flattening-filter-free (FFF) beam. Additionally, the treatment couch, with its specific material density and dimensions, was accurately modeled to reflect the patient's positioning during treatment.

Next, the ring-shaped spoilers, with a width of 7.0 cm, were positioned between the virtual patient (represented by the NIH phantoms) and the radiation source. The spoiler material was assigned a density of 1.185 g/cm^3 and atomic composition to realistically represent acrylic, the material used in the clinical settings. The spoiler's position within the TOPAS model was defined at a pre-determined distance from the patient surface,

mimicking the exact placement for a TBI treatment at the Tomotherapy machine. As already mentioned, standardized digital phantoms of a 15-year-old and a 35-year-old male -obtained from NIH were used in the TOPAS simulation to provide a realistic representation of the human body.

Additionally, a separate TOPAS simulation was performed for a modified ArcCHECK phantom, which was used in the actual experimental setup (see Section 2.2). The phantom includes additional inserts of Styrofoam to mimic the air in the lungs. Several X-ray CT scans[21] were taken for the modified ArcCHECK phantom. The DICOM data obtained from the CT scans were then included in the TOPAS simulation. This comprehensive virtual environment enabled one to perform detailed simulations and analyze how spoiler thickness impacts dose distribution within the phantoms and to compare the simulated results with that obtained from the experimental measurements.

In TOPAS, the Monte Carlo procedure tracks how the virtual particles within the simulation interact and deposit energy within the phantoms. This process is known as scoring (or tallying). By tracking the interactions of a large number of particles within specific volumes (e.g. voxels) or surfaces defined in the simulation geometry, quantities like particle flux and specific energy (i.e. absorbed dose) in each of the voxels and thus the dose distribution can be obtained.

A voxel grid was created with 254 bins along the X-direction with the bin size of 0.2137 cm, 127 bins along the Y-direction with the bin size of 0.2137 cm, and 222 bins along the Z-direction with the bin size of 0.8 cm. This level of detail was needed specifically for obtaining fine spatial dose distribution within the lungs. By scoring the

dose in the lung voxels, the impact of spoiler thickness variations on lung dose could be evaluated. Additionally, the dose distribution to the entire body, representing the target volume for TBI treatment, was also scored.

To achieve a balance between accuracy and computational efficiency, the number of simulated particles was carefully chosen. A total of 1×10^8 particles per degree were simulated for a full 360 degrees around the patient, resulting in a total particle histories of 3.6×10^{10}. This simulation generated a massive amount of data, with over 7.16 million voxels containing dose information. Due to the limitations of spreadsheet software like Excel, Python programming was utilized alongside a notepad editor to effectively manage and analyze all the data.

2.1.3 Analysis of TOPAS results

Following the TOPAS simulation of dose distribution within the phantoms, a detailed analysis of specific lung regions was conducted. A DICOM viewer was used to open and examine CT scans of the modified ArcCHECK phantom. This comparison aimed to identify suitable locations within the lungs for further investigation.

Within each lung across seven different CT scans, six specific points were chosen. The selection criteria leveraged data from the TOPAS simulation, particularly focusing on lung volume locations (at different Z-values) for each spoiler thickness. These points were strategically chosen to represent the dose distribution across various lung regions.

However, due to differing coordinate systems used in the TOPAS simulation (irradiation starting from the feet with Z = 0) and the DICOM CT scans (z = 0 representing

the head), a correction process was necessary. The Z-coordinate values were adjusted by using Z = 222-z, where z represents the z location in the DICOM while keeping the X and Y coordinates unchanged. This ensured that each dose value could be accurately matched with its corresponding location in the CT scans.

After matching dose values with their corresponding locations, the analysis focused on calculating an average lung dose. For each point within each lung and across all spoiler thicknesses, the dose values for the same X and Y coordinates but at different Z-values were averaged. These average dose values were then used to calculate an overall average dose for each point across different thicknesses. In total, 42 dose values were averaged for each lung. Subsequently, an average of these average doses across both lungs was calculated, encompassing a total of 84 well-distributed points in the right and left lung.

To determine the most effective spoiler thickness, the final average of all point doses within the lungs was employed as the primary metric. The spoiler thickness corresponding to the lowest average dose in both lungs was deemed the most effective one in minimizing lung exposure and achieving the highest skin dose.

This process was first performed without a spoiler to establish a baseline for comparison, which was then followed by a comprehensive analysis for each of the three spoiler thicknesses. A table summarizing the average dose for each lung, the average dose of the two lungs, and the skin dose for the various spoiler thicknesses was created. This facilitated the comparison among the results of the various spoiler thicknesses . Ultimately, the spoiler thickness with the lowest average dose of the lungs and the highest skin dose was identified as the optimal choice.

2.2 Experiment with the modified ArcCHECK phantom

2.2.1 Experimental set-up

The experiment with the modified ArcCHECK phantom was conducted at the Tomotherapy unit of the Augusta University Radiation Oncology Department in Augusta, Georgia at the Georgia Radiation Therapy Center. Figure 4 show the experimental setup.

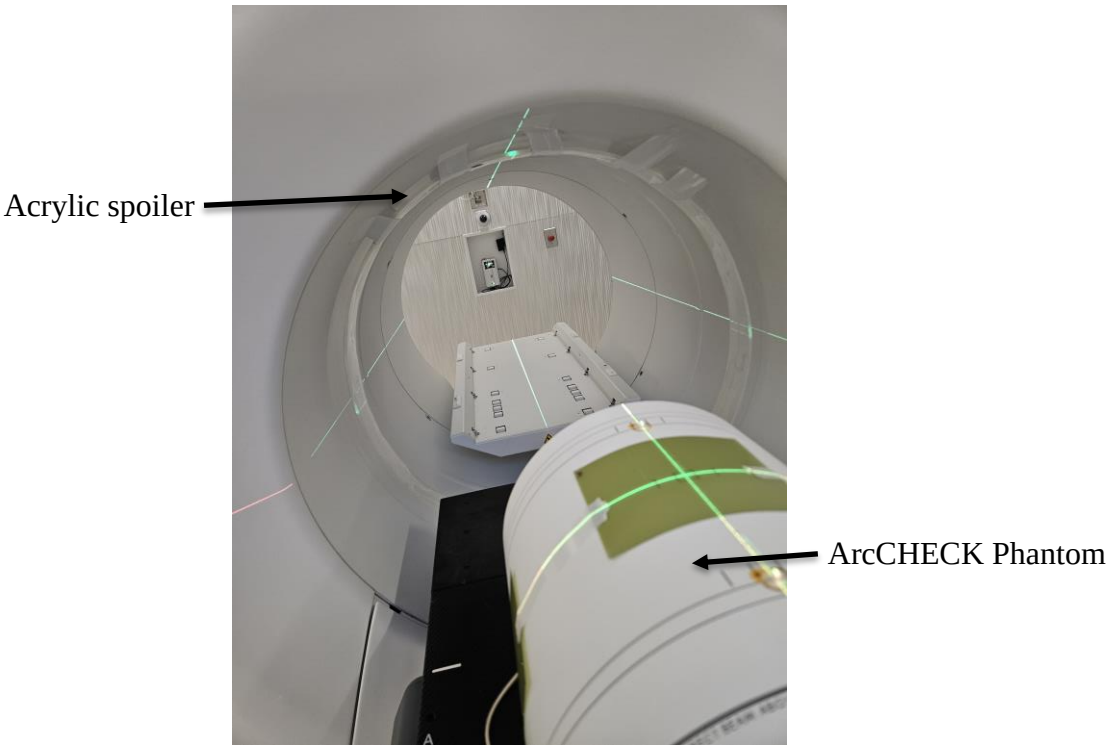

Figure 4 - Tomotherapy machine in the Radiation Therapy Center at Augusta University with the ArcCHECK phantom and a ring spoiler.

2.2.2 ArcCHECK

In addition to serve as a torso phantom, ArcCHECK (manufactured by Sun Nuclear) also includes an array of diode detectors serving as a critical instrument for quality

assurance (QA) for radiation therapy procedures. This tool functions by measuring and verifying various aspects of radiation delivery. It confirms the gantry angle, ensuring the treatment beam targets the intended area from the precise angle defined in the treatment plan. Additionally, it validates the accuracy of the multileaf collimator (MLC) blades responsible for shaping the radiation beam according to the plan. Furthermore, the ArcCHECK measures the actual dose distribution delivered by the linear accelerator (linac) during a treatment simulation. By comparing these measured values with the planned dose distribution, potential errors arising from miscalculations within the treatment planning system, mechanical issues with the linac, or inaccurate positioning of the MLC blades can be identified.

Beyond relative dose distribution measurement, the ArcCHECK offers additional functionalities that enhance treatment accuracy. It performs absolute dose calibration, ensuring that the dose delivered to the patient precisely matches the prescribed dose outlined in the treatment plan. The ArcCHECK also verifies treatment time, confirming that the entire planned dose is delivered within the intended timeframe.

As mentioned in Section 2.1.2 and shown in Figure 5, the modified ArcCHECK phantom includes additional inserts of Styrofoam. The low density of Styrofoam mimics the air in the lungs, which is invisible on CT scans. This allows for the placement of an ion chamber within the Styrofoam insert, enabling precise dose measurement at a specific point within the lung phantom. EBT3 films were sandwiched between the Styrofoam blocks as an additional set of measurements of the dose in the lungs. Lastly, EBT3 Films were taped/attached onto the outside surface of the ArcCHECK phantom (left, right, and middle) to measure the surface (or skin) dose.

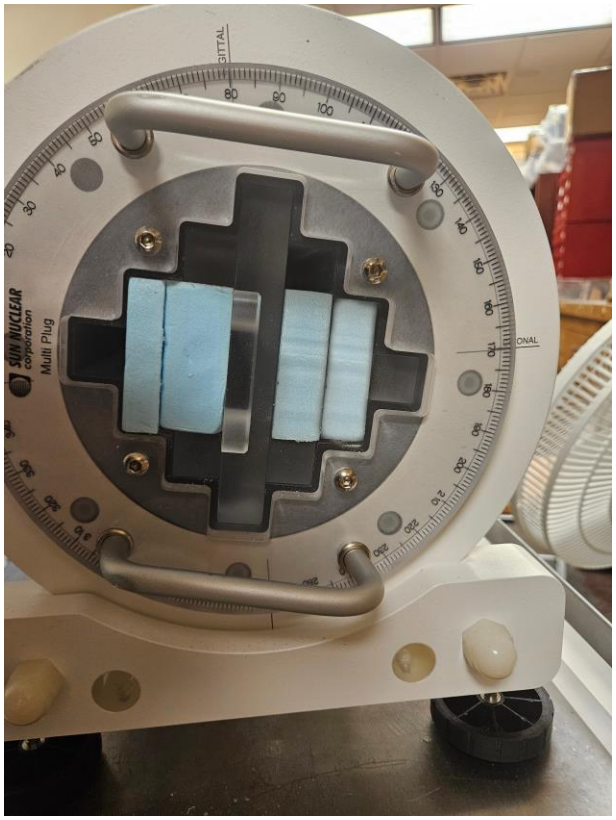

Figure 5. The modified ArcCHECK phantom including the Styrofoam blocks (blue) to mimic the air in the lungs.

The CT scans of the modified ArcCHECK phantom were used for treatment planning in RayStation 11A software. The lungs were designated as organs at risk, while the detector body and ion chamber were also contoured. Four treatment plans were created with the ion chamber positioned within the ArcCHECK. Different spoiler thicknesses (0 cm, 0.635 cm, 0.953 cm, and 1.588 cm) were placed between the ArcCHECK and the Tomotherapy machine to evaluate their impact on dose distribution. The diameter of the spoiler rings were approximately 82 cm, which fits snuggly inside the Tomotherapy machine.

Treatment plans were designed to deliver a dose of 200 cGy to the body while minimizing lung exposure. Specific treatment parameters were established, including projection time (0.327 seconds), number of projections (775), gantry rotation period (16.7 seconds), couch speed (0.089 cm/second), pitch factor (0.295), and field width (5.04 cm). The treatment plans using Raystation 11A are provided in Appendix A, Figures A1-A4, for the experiment with no spoiler and with a spoiler of various thicknesses.

Following irradiation of the modified ArcCHECK phantom with the ion chamber and EBT3 films for each spoiler[22,23,24] thickness, the collected ion chamber charge was converted to dose using a correction factor. The films were processed, scanned, and uploaded to RIT software for dose conversion. The average doses obtained from the films were then analyzed. Average doses for 4×4 cm^2 area were obtained from each film as shown in Figure 6. Analysis of the film data involved comparing average doses obtained from the three films that were placed on the outside surface of the ArcCHECK (ROI analysis) to identify the spoiler thickness resulting in the highest skin dose[25]. Similarly, average doses obtained from the films inserted between the Styrofoam blocks were compared to determine the spoiler thickness leading to the lowest lung dose.

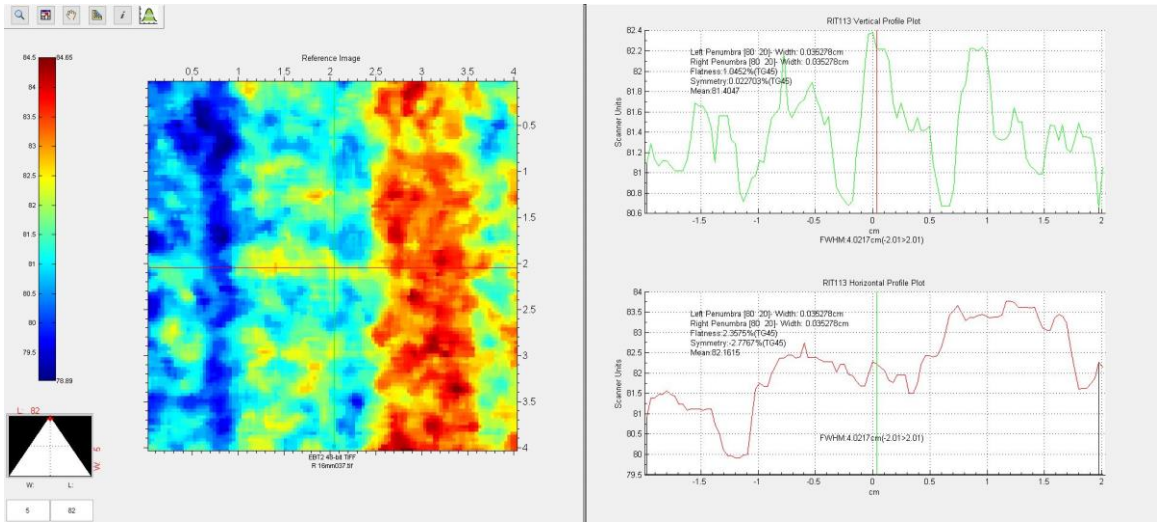
Reference Image
RIT113 Vertical Profile Plot
Left Penumbra (80_20)- Width: 0.035278cm
Right Penumbra (80_20)- Width: 0.035278cm
Flatness:1.0452%(TG45)
Symmetry:0.022703%(TG45)
Mean:81.4047
Scanner Units
cm
FWHM:4.0217cm(-2.01>2.01)
RIT113 Horizontal Profile Plot
Left Penumbra (80_20)- Width: 0.035278cm
Right Penumbra (80_20)- Width: 0.035278cm
Flatness:2.3575%(TG45)
Symmetry:-2.7767%(TG45)
Mean:82.1615
Scanner Units
cm
FWHM:4.0217cm(-2.01>2.01)

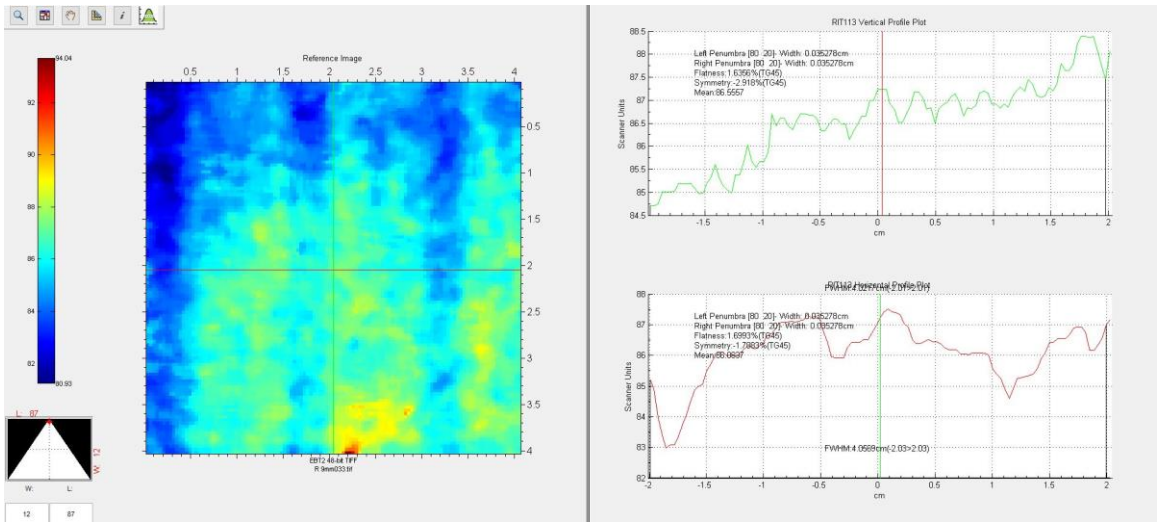
Reference Image
RIT113 Vertical Profile Plot
Left Penumbra (80_20)- Width: 0.035278cm
Right Penumbra (80_20)- Width: 0.035278cm
Flatness:1.6356%(TG45)
Symmetry:-2.918%(TG45)
Mean:86.5557
Scanner Units
cm
Left Penumbra (80_20)- Width: 0.035278cm
Right Penumbra (80_20)- Width: 0.035278cm
Flatness:1.6893%(TG45)
Symmetry:-1.7863%(TG45)
Mean:86.0807
Scanner Units
cm
FWHM:4.0569cm(-2.03>2.03)

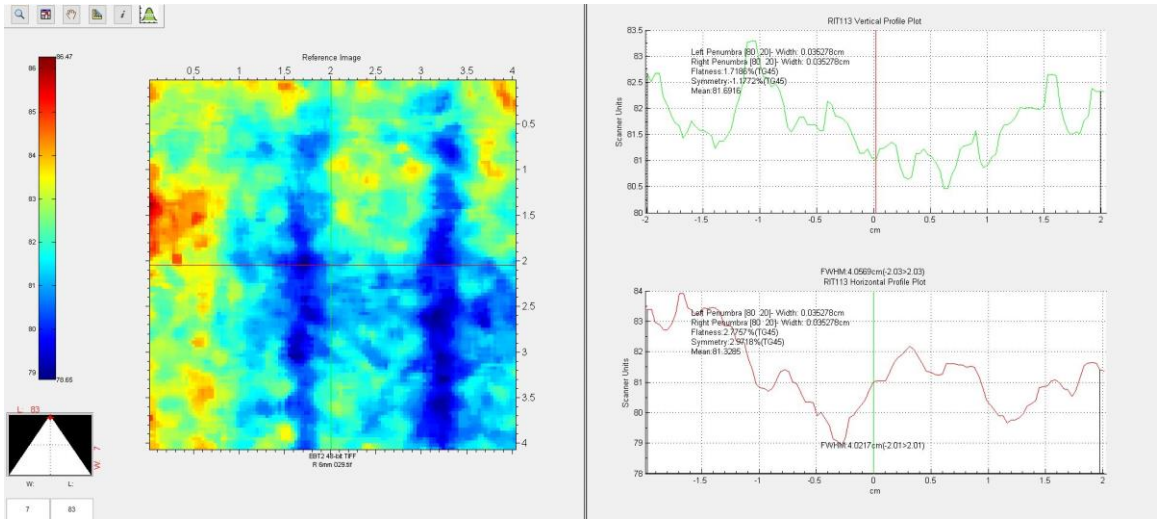
Reference Image
RIT113 Vertical Profile Plot
Left Penumbra (80_20)- Width: 0.035278cm
Right Penumbra (80_20)- Width: 0.035278cm
Flatness:1.7186%(TG45)
Symmetry:-1.1772%(TG45)
Mean:81.6916
Scanner Units
cm
FWHM:4.0569cm(-2.03>2.03)
RIT113 Horizontal Profile Plot
Left Penumbra (80_20)- Width: 0.035278cm
Right Penumbra (80_20)- Width: 0.035278cm
Flatness:2.7257%(TG45)
Symmetry:2.5718%(TG45)
Mean:81.3285
Scanner Units
cm
FWHM:4.0217cm(-2.01>2.01)

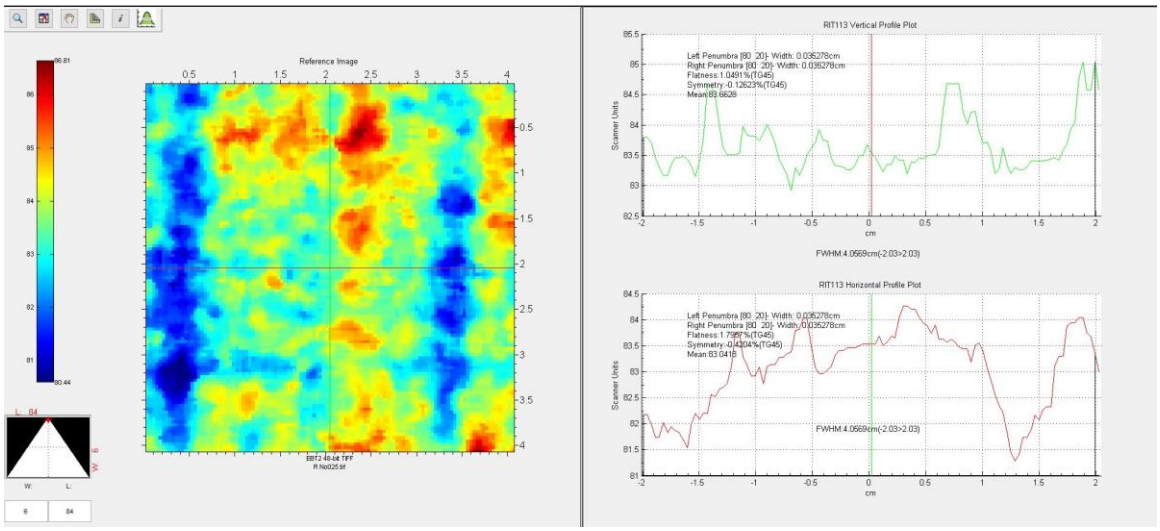

Figure 6. Average dose distribution for a 4x4 cm^2 area on a EBT3 Film for the right side skin dose using RIT software. The Figures are for different spoilers thicknesses (1.588, 0.953, 0.635, 0 cm) respectively.

Finally, the skin and lung dose results obtained from the TOPAS simulation were compared with the results obtained from the experiment to assess the accuracy of the TOPAS simulations in predicting lung dose distribution.

2.2.3 Dose calibration/conversion for EBT3 film

Since the EBT3 films do not directly measure the absorbed dose, one must experimentally establish an accurate calibration curve that converts the optical density (OD) of the film directly obtained from the film scanner readout to the absorbed dose. This was done by exposing the films with a field size of 7cm × 7cm and 100 cm source-to-surface distance (SSD), and a collimator angle of 45^o and 175 for Monitor Units (MU) to check the accuracy and the plan. Since the Tomotherapy machine includes a constantly moving MLCs, it does not provide a uniform radiation field. In order to accurately calibrate

the films, sixteen films were irradiated with a known dose using a Varian Edge linear accelerator. The irradiation parameters were meticulously selected to mimic the planned clinical setup for consistency. These parameters included a field size of 5cm × 5cm, 100 cm SSD, depth of 5 cm, backscatter of 5 cm, and beam energy of 6 MV FFF. Additionally, the monitor units (MU) were delivered at a rate matching the Tomotherapy machine (approximately 800 MU/min for the Edge vs. 1000 MU/min for the Tomotherapy).

Following irradiation, the films were kept away from light and radiation sources for 24 hours. Subsequently, the films were scanned using a flatbed scanner (an OD digitizer) to convert the OD distribution of the film to a set of numeric values with consistent settings maintained throughout the experiment (e.g., light source intensity, resolution). Specific regions of interest (ROIs) within the scanned film images were then chosen for OD measurement. This involved extracting average pixel values or net optical density (NOD) from the scanned data, where the OD is derived from the pixel values representing brightness.

Finally, the measured OD values (averaged across ROIs) were plotted against the corresponding known absorbed doses received during irradiation. This plot represents the film's response and serves as the calibration curve. By fitting an appropriate mathematical function, such as a polynomial, to this data, a reliable conversion between the OD and the absorbed dose can be achieved.

To ensure that the beam quality that was used in the EDGE machine by Varian matches the beam quality in the Tomotherapy machine. Ionization chambers were used to measure the dose profile of the beam at a reference plane. This profile depicts the lateral

and depth distribution of the dose within the beam and should match expected characteristics for a 6-MV FFF beam. An ion chamber was used to measure the charge collected using the Tomotherapy machine when delivering 100 cGy and the charge collected using the EDGE machine when delivering the same amount of dose. The charge collected for both machines had an excellent agreement of 1.7 nC.

CHAPTER III. RESULTS AND DISCUSSION

3.1 TOPAS results for the 35-year-old NIH male phantom irradiated with Tomotherapy beam

Figure 7 shows TOPAS results of the 2D normalized dose distribution of a 35-year-old NIH male phantom, where the points were selected inside the lungs and on the skin to calculate the corresponding doses for each spoiler thickness.

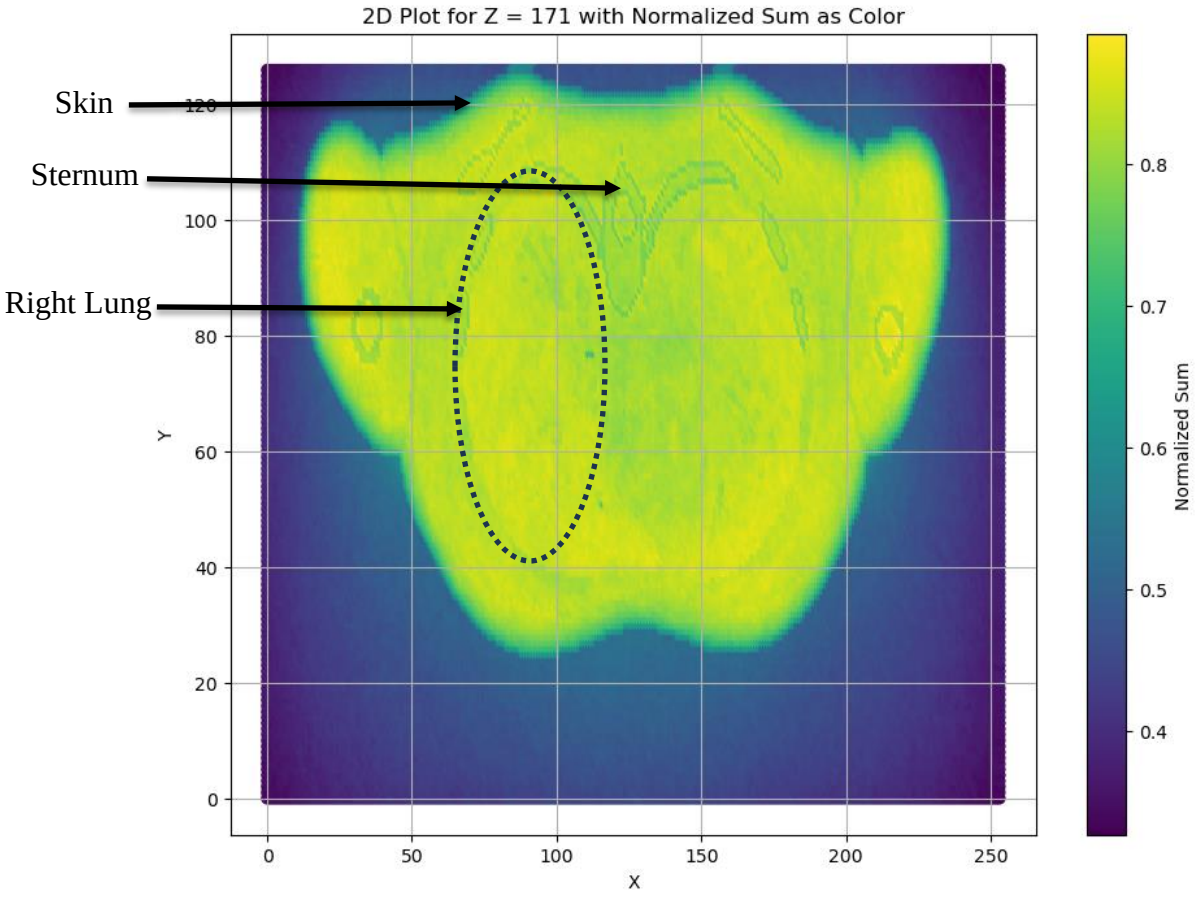

Figure 7. TOPAS results of a 2D normalized dose distribution of a 35-year-old NIH male phantom treated with 6-MV FFF Tomotherapy machine.

Table 1 presents the average lung and skin doses obtained from the TOPAS results for the various spoiler thicknesses. As described in Section 2.1.2, the results were based on the simulation of a total of 3.6×10^{10} source photons emitted from the 6-MV FFF Tomotherapy beam. The results indicate that the average lung dose decreases slightly as the spoiler thickness increases with the 1.588-cm spoiler yielded the lowest lung dose. This finding aligns with the expectation in that the spoilers with greater thicknesses attenuate the beam to a larger degree, leading to a reduction in the average lung dose. However, a higher surface dose is often preferred in procedures such as Bone Marrow Transplants (BMT), where it more effectively suppresses the immune system. Incidentally, Table 1 shows that the 1.588-cm spoiler also yields the highest average skin dose. This finding also aligns with the expectation (described in Section 1.4) that the electrons produced via Compton scattering events occurring in the spoiler would increase the skin dose. Therefore, the TOPAS results suggest that 1.588 cm is optimal among the three spoiler thicknesses being investigated.

Table 1. Average dose data for the 35-year-old NIH phantom based on the TOPAS results.

Spoiler Thickness (cm)	0	0.635	0.953	1.588
Right Lung Average Dose (E-5 cGy)*	4.49	4.43	4.39	4.33
Left Lung Average Dose (E-5 cGy)*	4.45	4.40	4.37	4.32
Average Total Lung Dose (E-5 cGy)*	4.47	4.41	4.38	4.32
Average Skin Dose (E-5 cGy)**	3.06	3.53	3.71	3.87

*: Dose data for the lungs has a Standard Deviation (SD) of less than 1.21%.
**: Dose data for the skin has a SD of 10%.

3.2 TOPAS results for ArcCHECK phantom irradiated with Tomotherapy beam

Table 2 presents the average lung and skin doses, and the dose in the ion chamber, obtained from the TOPAS results for the ArcCHECK phantom irradiated with the various spoiler thicknesses. Same as that in Table 1, the results in Table 2 were also based on the simulation of a total of 3.6×10^{10} source photons emitted from the 6-MV FFF Tomotherapy beam. The results show that the average lung doses are approximately 20% lower than that shown in Table 1 and that they remain more-or-less the same (i.e. within statistical uncertainties) for various spoiler thicknesses. The lower doses can be explained by the fact that the lung locations defined in the ArcCHECK phantom are deeper than those in the 35-year-old NIH phantom. The skin dose results in Table 2 are consistent with the Table 1 results in that the highest skin dose corresponds to the 1.588-cm spoiler.

Table 2. Average dose data for ArcCHECK based on the TOPAS results.

Spoiler thickness (cm)	0	0.635	0.953	1.588
Right lung average dose (E-5 cGy)*	3.65	3.62	3.58	3.52
Left lung average dose (E-5 cGy)*	3.41	3.61	3.54	3.55
Average dose of lungs (E-5 cGy)*	3.53	3.61	3.56	3.54
Skin dose (E-5 cGy)**	2.02	2.67	2.88	3.11
Average ion chamber dose (E-5 cGy)*	3.40	3.31	3.34	3.45

*: Dose data for the lungs has a Standard Deviation (SD) of less than 1%.
**: Dose data for the skin has a SD of 9%.

3.3 Experimental results for the ArcCHECK phantom irradiated with Tomotherapy beam

Table 3 shows the doses that were delivered to the sixteen EBT3 films and the corresponding OD values. As shown, the dose monotonically increases with the OD. The relationship between the dose and the OD value is further illustrated via the dose-to-OD conversion curve shown in Figure 8.

Table 3. Data used for setting the dose-to-OD conversion curve.

Film	Dose (cGy)	OD value
1	0	24025.39
2	10	24751.27
3	15	25067.03
4	20	25704.67
5	40	26270.79
6	50	27184.79
7	60	27825.41
8	100	29365.92
9	120	30333.08
10	140	34081.7
11	160	34748.07
12	180	35707.96
13	200	38166.33
14	220	38889.35
15	240	40477.82

16	260	42039.02

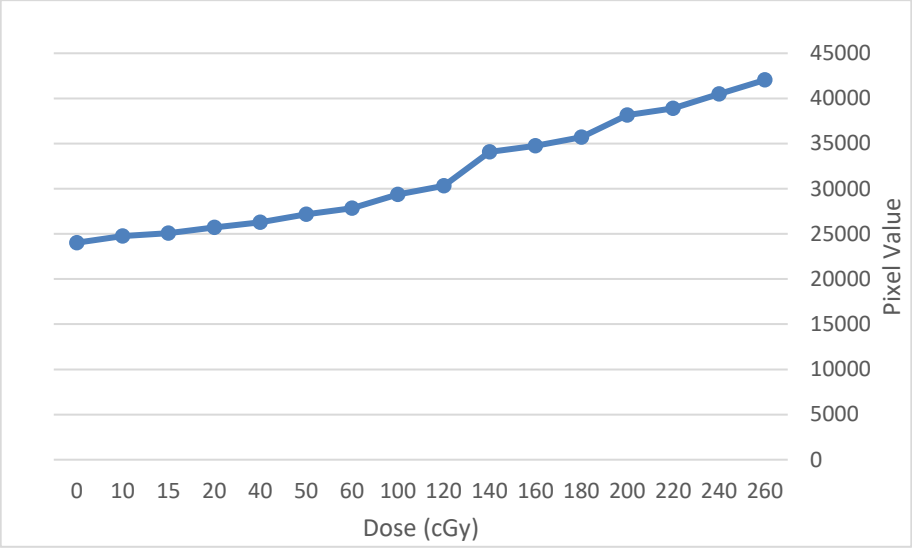

Figure 8. Dose-to-OD conversion curve.

Table 4 shows the measured dose data (from EBT3 films) for the modified ArcCHECK phantom irradiated with the 6-MV FFF Tomotherapy beam. Consistent with the results from TOPAS simulations for both the 35-year-old male phantom and the modified ArcCHECK phantom, the 1.588-cm spoiler yielded the lowest average lung dose, likely due to the slightly more beam attenuation. However, discrepancies exist regarding the measured skin dose data in two aspects. First, the measured skin doses remain more-or-less the same (within statistical uncertainties) for various spoiler thicknesses and having an air gap between the spoiler and the Tomotherapy machine. Second, the measured skin dose values were about one half that of the lung doses. This may be explained by the fact that the electrons produced in the spoiler are spread out and deposit their energies in a

larger area than the area occupied by the EBT3 film on the ArcCHECK surface. At the surface of the phantom where the skin dose was measured there was no Charged-Particle Equilibrium (CPE).

Table 4. The measured dose data (from EBT3 films) for the modified ArcCHECK phantom irradiated with the 6-MV FFF Tomotherapy beam.

Spoiler thickness (cm)	0	0.635	0.953	1.588
Lung Dose (cGy)	174	166	166	163
Skin Dose (cGy)	82.4	84.8	84	82.1

Finally, regarding the ion chamber calibration factor used to convert measured charge to actual dose: three measurements were performed, yielding an average collected charge of 15.287 nC. Equation 1 was subsequently employed to calculate the calibration factor in cGy/nC.

$$Calibration\ Factor = \frac{Dose}{Charge\ Collected} \quad (1)$$

For a dose of 82.7 cGy that was delivered using 1400 Monitor Units with 100 SSD, a calibration factor of 5.41 cGy/nC was calculated, that was used to convert the charge collected in each spoiler thickness case to dose.

Table 5. Dose measured by the ion chamber.

Spoiler Thickness (cm)	Charge (nC)	Dose (cGy)	Error Percentage
0	39.74	214	-0.46
0.635	38.27	206	0.5
0.953	37.56	203	0.1
1.588	36.26	196	-0.11

The lowest dose measured by the ion chamber was obtained with the 1.588-cm spoiler. This finding aligns with both the average lung dose data from TOPAS simulations and the ArcCHECK lung dose measurements using film detectors. Furthermore, the ion chamber measurements demonstrated good agreement with the dose calculated by the treatment planning system, exhibiting a maximum discrepancy of only 0.5%.

CHAPTER IV. CONCLUSIONS AND FUTURE WORK

Tomotherapy machine offers a valuable tool for TBI for immunosuppression in certain patient populations. However, achieving optimal dose distribution presents challenges. One challenge is minimizing lung dose while achieving an adequate skin dose. Adding a ring-shaped spoiler of an appropriate thickness is a way to achieve the dose requirements.

The TOPAS simulation results of this study for both the 35-year-old NIH phantom and the ArcCHECK phantom show that the thickest (1.588-cm) spoiler yielded the lowest lung dose and the highest skin dose. This conclusion is further supported by the experimentally obtained dose data from the EBT3 films that were mounted on the ArcCHECK phantom and irradiated with the Tomotherapy machine. The ion chamber measurements within the ArcCHECK system demonstrated good agreement with the TPS calculations, exhibiting a maximum error of only 0.5% for lung dose. Furthermore, the dose data measured with the ion chamber also show that lowest lung dose was achieved with the thickest spoiler.

For future studies, improvements should be made to more accurately simulate the MLCs pattern according to the treatment plan. In addition, the discrepancy of the measured skin dose for the experimental modified ArcCHECK phantom can be further investigated.

APPENDIX A

ARCCHECK TREATMENT PLANS

The treatment plans were made using Raystation 11A, the focus was reducing the lung dose while achieving a high skin dose. Figures A1-A4 show the treatment plans for ArcCHECK treatment with no spoiler and with a spoiler of various thicknesses.

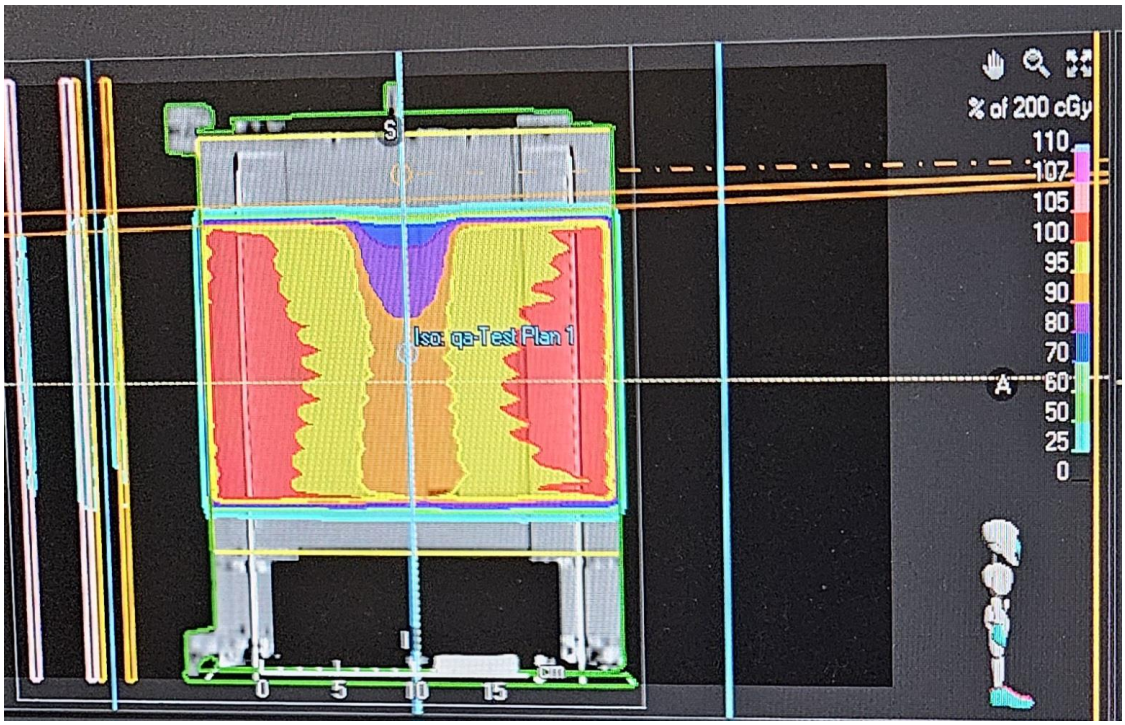

Figure A1- ArcCHECK Treatment plan with no spoiler.

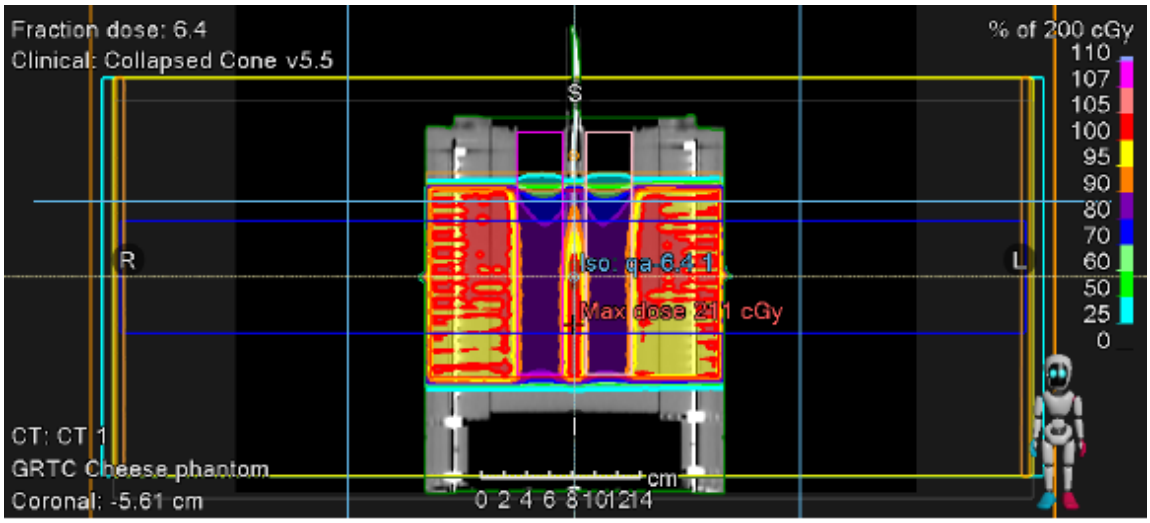

Figure A2- ArcCHECK Treatment plan with a 0.635-cm spoiler.

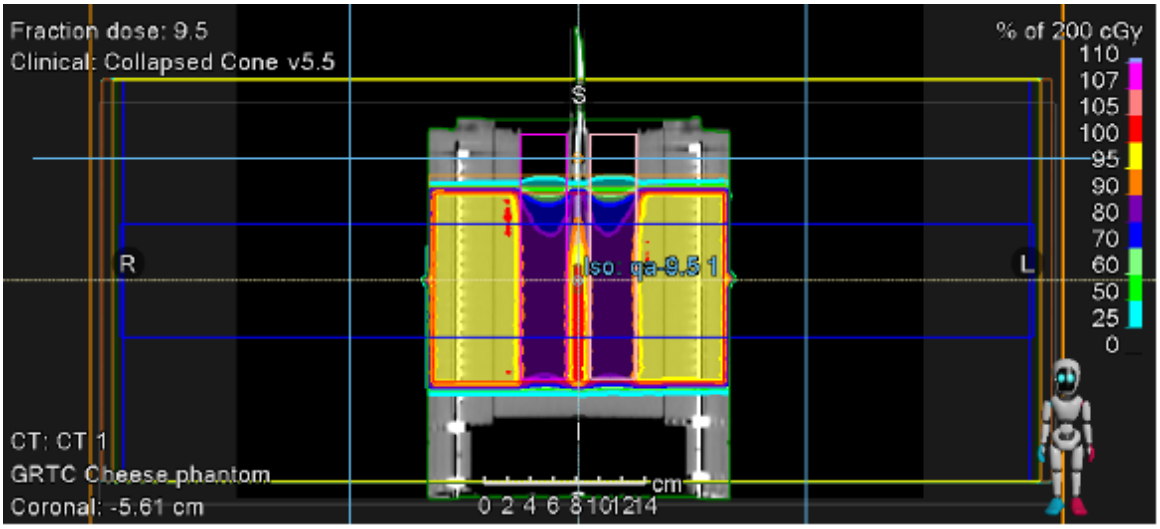

Figure A3 - ArcCHECK Treatment plan with a 0.953-cm spoiler.

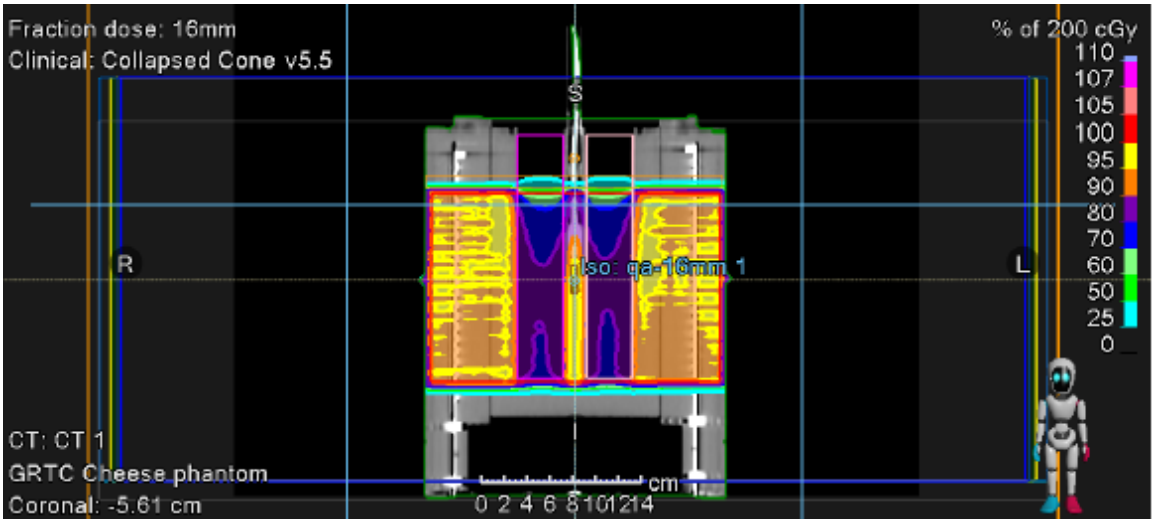

Figure A4- ArcCHECK Treatment plan with a 1.588-cm spoiler.

REFERENCES

1. Quast U. Whole body radiotherapy: A TBI-guideline. J Med Phys. 2006 Jan;31(1):5-12. doi: 10.4103/0971-6203.25664. PMID: 21206634; PMCID: PMC3003894.

2. American Association of Physicists in Medicine. Task Group 29 (J. Van Dyk, Chair, J. M. Galvin, G. P. Glasgow, & E. B. Podgorsak). (1986, June). The physical aspects of total and half body photon irradiation.

3. Choi DH, Ahn SH, Park K, Choi SH, Kim JS. Development of Total Lymphoid Irradiation (TLI)-Dedicated Shielding and Image-Guided System and Dose Evaluation Using 3D-Printed Rat Phantom. Front Vet Sci. 2022 May 18;9:832272. doi: 10.3389/fvets.2022.832272. PMID: 35664845; PMCID: PMC9159376.

4. Hoeben BAW, Wong JYC, Fog LS, Losert C, Filippi AR, Bentzen SM, Balduzzi A, Specht L. Total Body Irradiation in Haematopoietic Stem Cell Transplantation for Paediatric Acute Lymphoblastic Leukaemia: Review of the Literature and Future Directions. Front Pediatr. 2021 Dec 3;9:774348. doi: 10.3389/fped.2021.774348. PMID: 34926349; PMCID: PMC8678472.

5. Vogel J, Hui S, Hua CH, Dusenbery K, Rassiah P, Kalapurakal J, Constine L, Esiashvili N. Pulmonary Toxicity After Total Body Irradiation - Critical Review of the Literature and Recommendations for Toxicity Reporting. Front Oncol. 2021 Aug 26;11:708906. doi: 10.3389/fonc.2021.708906. PMID: 34513689; PMCID: PMC8428368.

6. Jenkin,R.D.T., Rider, W.D., Sonley, M.H. Ewing's sarcoma: A trial of adjuvant total body irradiation. Radiology. 96, 151-155. 1970.

7. Fitzpatrick, P.J., Rider, W.D. Half body radiotherapy. Int. J.Radiat. Oncol. Biol. Phys. 1, 197-207, 1976.

8. Langen, K. M., Papanikolaou, N., Balog, J., Crilly, R., Followill, D., Goddu, S. M., ... Shi, C. (2010, August). QA for helical tomotherapy: Report of the AAPM Task Group 148. Medical Physics, 37(9), 4817-4853.

9 . Lee J, Kim E, Kim N, Suh CO, Chung Y, Yoon HI. Pulmonary toxicity of craniospinal irradiation using helical tomotherapy. Sci Rep. 2022 Feb 25;12(1):3221. doi: 10.1038/s41598-022-07224-1. PMID: 35217707; PMCID: PMC8881492.

10. Berumen F, Ma Y, Ramos-Méndez J, Perl J, Beaulieu L. Validation of the TOPAS Monte Carlo toolkit for HDR brachytherapy simulations. Brachytherapy. 2021 Jul-Aug;20(4):911-921. doi: 10.1016/j.brachy.2020.12.007. Epub 2021 Apr 23. PMID: 33896732.

11. Lee H, Cheon BW, Feld JW, Grogg K, Perl J, Ramos-Méndez JA, Faddegon B, Min CH, Paganetti H, Schuemann J. TOPAS-imaging: extensions to the TOPAS simulation toolkit for medical imaging systems. Phys Med Biol. 2023 Apr 3;68(8):10.1088/1361-6560/acc565. doi: 10.1088/1361-6560/acc565. PMID: 36930985; PMCID: PMC10164408.

12. Kang SK, Cho BC, Park SH, Park HC, Bae H, Kim JO, Keall PJ, Siebers JV. Monte Carlo-based treatment planning for a spoiler system with experimental validation using plane-parallel ionization chambers. Phys Med Biol. 2004 Nov 21;49(22):5145-55. doi: 10.1088/0031-9155/49/22/009. PMID: 15609564.

13. Hurtado J, Lee C, Lodwick D, Goede T, Williams JL, Bolch WE. Hybrid computational phantoms representing the reference adult male and adult female: construction and applications for retrospective dosimetry. Health Phys. 2012 Mar;102(3):292-304. doi: 10.1097/HP.0b013e318235163f. PMID: 22315022; PMCID: PMC3859249.

14. Lee C, Lodwick D, Williams JL, Bolch WE. Hybrid computational phantoms of the 15-year male and female adolescent: applications to CT organ dosimetry for patients of variable morphometry. Med Phys. 2008 Jun;35(6):2366-82. doi: 10.1118/1.2912178. PMID: 18649470; PMCID: PMC2809721.

15. Chapman D, Barnett R, Yartsev S. Helical tomotherapy quality assurance with ArcCHECK. Med Dosim. 2014 Summer;39(2):159-62. doi: 10.1016/j.meddos.2013.12.002. Epub 2014 Jan 13. PMID: 24433834.

16. Petoukhova AL, van Egmond J, Eenink MG, Wiggenraad RG, van Santvoort JP. The ArcCHECK diode array for dosimetric verification of HybridArc. Phys Med Biol. 2011 Aug 21;56(16):5411-28. doi: 10.1088/0031-9155/56/16/021. Epub 2011 Jul 29. PMID: 21804180.

17. Bassi S, Cummins D, McCavana P. Energy and dose dependence of GafChromic EBT3-V3 film across a wide energy range. Rep Pract Oncol Radiother. 2020 Jan-Feb;25(1):60-63. doi: 10.1016/j.rpor.2019.12.007. Epub 2019 Dec 9. PMID: 31889923; PMCID: PMC6931201

18. Villarreal-Barajas JE, Khan RF. Energy response of EBT3 radiochromic films: implications for dosimetry in kilovoltage range. J Appl Clin Med Phys. 2014 Jan 6;15(1):4439. doi: 10.1120/jacmp.v15i1.4439. PMID: 24423839; PMCID: PMC5711253.

19. Chen SK, Hollender L. Digitizing of radiographs with a flatbed scanner. J Dent. 1995 Aug;23(4):205-8. doi: 10.1016/0300-5712(95)91183-n. PMID: 7629323.

20. Shin SS, Ahn S, Baek SH, Kwak J, Kim JS, Ahn WS. Usefulness of Semi-cylindrical Beam Spoiler in Treatment of Early Glottic Cancer Using 6 MV Photon Beam. In Vivo. 2022 Jan-Feb;36(1):465-472. doi: 10.21873/invivo.12726. PMID: 34972750; PMCID: PMC8765191.

21. Davis AT, Palmer AL, Nisbet A. Can CT scan protocols used for radiotherapy treatment planning be adjusted to optimize image quality and patient dose? A systematic review. Br J Radiol. 2017 Aug;90(1076):20160406. doi: 10.1259/bjr.20160406. Epub 2017 May 23. PMID: 28452568; PMCID: PMC5603945.

22. Niroomand-Rad A, Javedan K, Rodgers JE, Harter KW. Effects of beam spoiler on radiation dose for head and neck irradiation with 10-MV photon beam. Int J Radiat Oncol Biol Phys. 1997 Mar 1;37(4):935-40. doi: 10.1016/s0360-3016(96)00538-x. PMID: 9128972

23. Klein EE, Michalet-Lorenz M, Taylor ME. Use of a lucite beam spoiler for high-energy breast irradiation. Med Dosim. 1995 Summer;20(2):89-94. doi: 10.1016/0958-3947(95)00006-i. PMID: 7632350.

24. Kassaee A, Bloch P, Yorke E, Altschuler MD, Rosenthal DI. Beam spoilers versus bolus for 6 MV photon treatment of head and neck cancers. Med Dosim. 2000 Fall;25(3):127-31. doi: 10.1016/s0958-3947(00)00038-8. PMID: 11025258.

25. Friend BD, Bailey-Olson M, Melton A, Shimano KA, Kharbanda S, Higham C, Winestone LE, Huang J, Stieglitz E, Dvorak CC. The impact of total body irradiation-based regimens on outcomes in children and young adults with acute lymphoblastic leukemia undergoing allogeneic hematopoietic stem cell transplantation. Pediatr Blood Cancer. 2020 Feb;67(2):e28079. doi: 10.1002/pbc.28079. Epub 2019 Nov 14. PMID: 31724815.